

| | | | | | |
|--|------------------------------------|-------------------------------------|--|--|---|
| REPORT DOCUMENTATION PAGE | | | | Form Approved OMB No. 0704-0188 | |
| Public reporting burden for this collection of information is estimated to average 1 hour per response, including the time for reviewing instructions, searching existing data sources, gathering and maintaining the data needed, and completing and reviewing this collection of information. Send comments regarding this burden estimate or any other aspect of this collection of information, including suggestions for reducing this burden to Department of Defense, Washington Headquarters Services, Directorate for Information Operations and Reports (0704-0188), 1215 Jefferson Davis Highway, Suite 1204, Arlington, VA 22202-4302. Respondents should be aware that notwithstanding any other provision of law, no person shall be subject to any penalty for failing to comply with a collection of information if it does not display a currently valid OMB control number. PLEASE DO NOT RETURN YOUR FORM TO THE ABOVE ADDRESS. | | | | | |
| 1. REPORT DATE (DD-MM-YYYY) 24-02-1998 | | 2. REPORT TYPE Paper | | 3. DATES COVERED (From - To) | |
| 4. TITLE AND SUBTITLE Progress Towards the Production of Cryosolid HEDM Samples by Laser Ablation and Matrix Isolation Techniques | | | | 5a. CONTRACT NUMBER | |
| | | | | 5b. GRANT NUMBER | |
| | | | | 5c. PROGRAM ELEMENT NUMBER | |
| 6. AUTHOR(S) Mario E. Fajardo; Michel Macler; Simon Tam | | | | 5d. PROJECT NUMBER 2303 | |
| | | | | 5e. TASK NUMBER M2C8 | |
| | | | | 5f. WORK UNIT NUMBER | |
| 7. PERFORMING ORGANIZATION NAME(S) AND ADDRESS(ES) AND ADDRESS(ES) Air Force Research Laboratory (AFMC) AFRL/PRSP 5 Pollux Drive Edwards AFB CA 93524-7048 | | | | 8. PERFORMING ORGANIZATION REPORT | |
| 9. SPONSORING / MONITORING AGENCY NAME(S) AND ADDRESS(ES) Air Force Research Laboratory (AFMC) AFRL/PRS 5 Pollux Drive Edwards AFB CA 93524-7048 | | | | 10. SPONSOR/MONITOR'S ACRONYM(S) | |
| | | | | 11. SPONSOR/MONITOR'S NUMBER(S) AFRL-PR-ED-TP-1998-049 | |
| 12. DISTRIBUTION / AVAILABILITY STATEMENT Approved for public release; distribution unlimited. | | | | | |
| 13. SUPPLEMENTARY NOTES | | | | | |
| 14. ABSTRACT | | | | | |
| 15. SUBJECT TERMS | | | | | |
| 16. SECURITY CLASSIFICATION OF: | | | 17. LIMITATION OF ABSTRACT A | 18. NUMBER OF PAGES | 19a. NAME OF RESPONSIBLE PERSON P. Carrick |
| a. REPORT Unclassified | b. ABSTRACT Unclassified | c. THIS PAGE Unclassified | | | 19b. TELEPHONE NUMBER (include area code) (661) 275-4481 |

HIGH ENERGY DENSITY MATTER (HEDM) CONTRACTORS' CONFERENCE
Chantilly, VA 1-3 June 1997

**Progress Towards the Production of Cryosolid HEDM Samples by
Laser Ablation and Matrix Isolation Techniques**

Mario E. Fajardo, Michel Macler, and Simon Tam

Propulsion Sciences Division, Propulsion Directorate, Phillips Laboratory
(OLAC PL/RKS Bldg. 8451, Edwards AFB, CA 93524-7680)

ABSTRACT

We report a newly developed method for rapid in-vacuum deposition of thick solid parahydrogen (pH₂) samples which are remarkable for their excellent optical qualities. These experiments were driven by the technological requirement of scaling up HEDM sample production while retaining the desirable aspects of the matrix isolation method for introducing energetic dopants (simplicity, versatility, etc.). The scientific result is a pronounced improvement in the quality of spectroscopic information obtained from these millimeters thick pH₂ samples.

Infrared absorption spectra of pure pH₂ samples suggests a hexagonal close-packed (hcp) microscopic structure[§]. The excellent optical and thermal properties suggest an overall polycrystalline structure, with large (~ 1 mm ?) crystallites.

We have obtained clean, reproducible spectra of the 200-220 nm electronic absorptions of B atoms in pH₂. We have observed the infrared (IR) absorptions of several molecular species produced either directly by ablation (*e.g.* carbon clusters) or by reactions with the matrix host. We have also observed a variety of novel induced IR absorptions of the pH₂ matrix host itself; transitions induced by the presence of atoms, molecules, and ions.

These results constitute the most important scientific and technological advances achieved by our group over the past few years. We expect significant impacts both on the field of condensed phase spectroscopy, and on the prospects of producing useful quantities of HEDM doped cryosolid propellants.

[§] Throughout the text this symbol refers the reader to the Addendum following the References.

INTRODUCTION

Our previous efforts at using optical absorption spectroscopy to demonstrate the trapping of Li, B, Na, Mg, and Al atoms in cryogenic solid hydrogen matrices [refs. 1-3] have been made all the more difficult by the strong optical scattering properties of vapor deposited hydrogen films [ref. 4]. Such films are typically polycrystalline, with microcrystallites having dimensions comparable to optical wavelengths; the optical scattering results from abrupt changes in the solid's refractive index at microcrystallite boundaries. In the ultraviolet (UV) spectral region, e.g.: $\lambda \approx 0.2 \mu\text{m}$, optical scattering losses can easily exceed 90% in vapor deposited normal hydrogen films only $\sim 10 \mu\text{m}$ thick (normal hydrogen, nH_2 , is the room temperature equilibrium mixture of 75% ortho hydrogen $\{\text{oH}_2\}$ and 25% para hydrogen $\{\text{pH}_2\}$ [ref. 5]). Absorption spectra of dopant species obtained from such matrices suffer from poor signal-to-noise ratios and wavelength dependent baseline correction errors.

Our first approach to producing transparent solid hydrogen matrices involved cooling and converting the hydrogen host gas to nearly pure (99.99%) pH_2 by passing room temperature nH_2 gas through a cold (15 K) catalyst bed, followed immediately by deposition of the pH_2 onto a 2 K substrate [refs. 6, 7 and *vide infra*]. Unfortunately, matrices deposited in this manner at conventional matrix host gas flow rates of $\sim 1 \text{ mmol/hr}$ still exhibited significant optical scattering. Because of the strong wavelength dependence of the scattering phenomenon [ref. 8] the losses are less dramatic in the infrared (IR) spectral region than in the UV, but are still a nuisance. For example, a $\approx 50 \mu\text{m}$ thick pH_2 matrix deposited at $\sim 1 \text{ mmol/hr}$, doped with C_n and hydrocarbon species by laser ablation of graphite, exhibited scattering losses of $\approx 20\%$ at $\lambda = 2.0 \mu\text{m}$ [ref. 7].

Motivated by the technological requirement of establishing the scaling characteristics of HEDM sample production techniques, we recently attempted a number of pH_2 depositions at host gas flow rates of 10 to 200 mmol/hr. We anticipated great difficulties in performing absorption experiments in these thicker samples. However, we were pleasantly surprised to find that the resulting millimeters thick solid hydrogen samples are amazingly transparent even at vacuum UV wavelengths! We speculate that the higher deposition rates somehow allow for "self-annealing" of the accreting surface of the matrix during deposition, resulting in larger and fewer crystallites, and hence in greatly reduced optical scattering. Furthermore, and potentially of great significance to both the HEDM cryosolid effort and to matrix isolation spectroscopy in general, we have

demonstrated the trapping and isolation of numerous atomic, molecular, and ionic species in these rapidly deposited samples.

In what follows we describe: (1) the new experimental apparatus and sample preparation conditions, (2) demonstration of control over the ortho:para ratio of the hydrogen matrix host, (3) the remarkable optical, thermal, and spectroscopic properties of these rapidly deposited samples, (4) UV and IR absorption spectra of trapped B atoms and C_n molecules, respectively, and finally (5) novel IR absorptions of the H_2 host itself induced by the presence of atomic, molecular, and charged dopants.

EXPERIMENTAL

We employ an ortho-to-para hydrogen converter consisting of an 1/8 inch OD by 1.5 m long copper tube packed with 1.4 g of APACHI catalyst [ref. 5] wound and potted with conductive epoxy onto a copper bobbin (Figure 1) which can be cooled to below 10 K by a closed-cycle cryostat. This setup allows for continuous H_2 flow rates at 15 K in excess of 1 mol/hr, yielding a flow of pre-cooled 99.99% pH_2 which is deposited directly onto a BaF_2 substrate cooled to 2 K by a separate liquid helium bath cryostat (Figure 2). Because of the sample-in-vacuum design of our cryostat, sample thickness growth rates are limited to < 1 cm/hour by the pumping speed of the small turbomolecular pump which maintains the

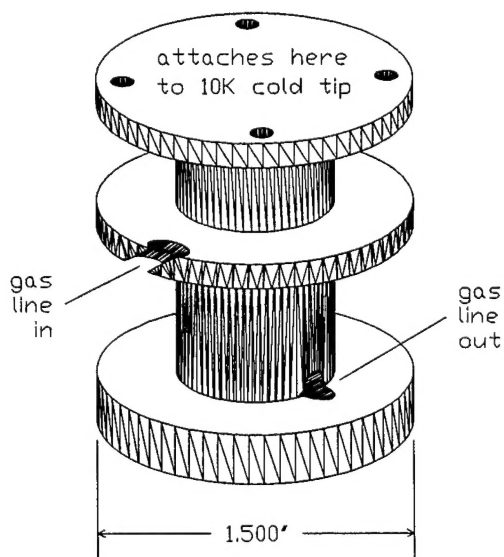


Figure 1. ortho/para Converter Bobbin.

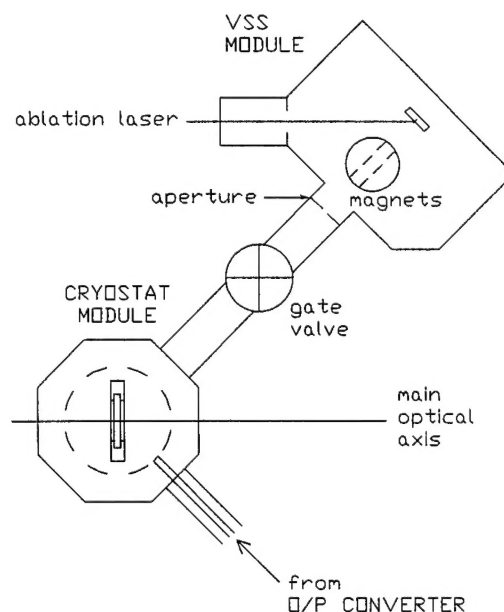


Figure 2. Experimental Schematic.

cryogenic thermal isolation vacuum ($P < 10^{-4}$ Torr uncondensed H_2 required to avoid thermal runaway); ultimate sample thickness is limited by the 3 liter capacity of the liquid helium bath cryostat. The uncondensed H_2 results in an additional complication: the deposition of a second solid H_2 film on the back side of the BaF_2 substrate, amounting to 8 to 9% of the main front side sample thickness; this front:back thickness ratio is independent of H_2 inlet flow rate.

Figure 2 also depicts the arrangement of our laser ablation dopant source. The Temporally and Spatially Specific PhotoIonization (TASSPI) Velocity Selected Source (VSS) module [refs. 9-12] is attached to the deposition chamber of our liquid helium bath cryostat. While no velocity selected atomic depositions are reported in this manuscript, it is important to note that the VSS module includes a pair of removable magnets which can be used to eliminate charged species from the laser ablated plume. For depositions in which the dopants are volatile at room temperature, such as CO, N_2 , and CH_3OH , the VSS module was replaced by a simple copper tube inlet connecting the deposition chamber with a separate gas handling manifold.

Back-reflection HeNe laser interferograms taken during deposition, and matrix UV and IR absorption spectra, are obtained along the main optical axis. These diagnostics simultaneously probe both front and back side H_2 samples. To accommodate the IR diagnostic, most of the apparatus resides inside a 0.5 m^3 polycarbonate box purged with a constant flow of dry N_2 gas.

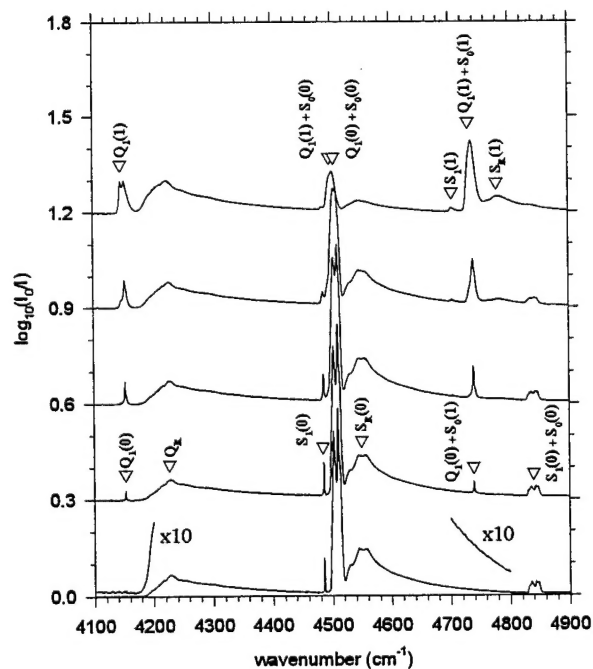


Figure 3. Ortho/para composition of $\approx 0.9\text{ mm}$ total (front + back) thickness vapor deposited solid hydrogen samples at $T = 2\text{ K}$. The oH_2 concentrations increase from bottom to top in the sequence: 0.01%, 2%, 8%, 25%, and 70%, corresponding to o/p converter bobbin temperatures of: 15 K, 28 K, 37 K, 52 K, and 135 K. In each case $\approx 55(\pm 3)$ mmol of hydrogen were deposited in a 1 hour period. The absence in the bottom trace of the $Q_1(0)$ (4153 cm^{-1}) and $Q_1(0)+S_0(1)$ (4740 cm^{-1}) absorptions is evidence of the very low oH_2 concentration ($< 0.1\%$) in that sample. The spectra are presented at 1 cm^{-1} FWHM resolution.

RESULTS AND DISCUSSION

Figure 3 shows absorption spectra ($A = \log_{10}[I_0/I]$) of five different rapidly deposited solid hydrogen samples, of different oH₂ compositions obtained by adjusting the temperature of the ortho/para converter bobbin. Infrared activity in the homonuclear diatomic H₂ molecules arises from dipoles induced by intermolecular interactions in the condensed phase environment [refs. 13, 14]. The observed spectral changes with increasing oH₂ concentrations match exactly those reported for solid hydrogen crystals grown from the liquid [ref. 15]. None of these samples exhibited appreciable optical scattering, either visually or in the form of a wavelength dependent scattering background across the 1000 to 5000 cm⁻¹ range.

Figure 4 shows the linearity of the sample thickness growth rates for two of the highest H₂ inlet flow rates used in this study. Both traces show similar ratios of H₂ host gas inlet amount to final total (back + front) sample thickness of about 60(±5) mmol/mm, the same as for the slower

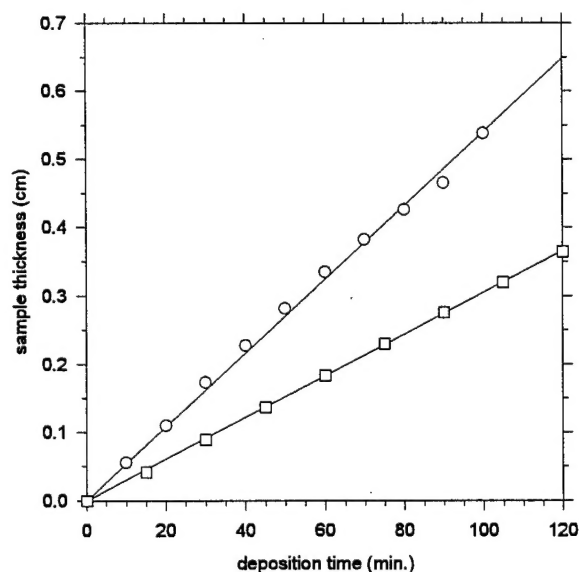


Figure 4. Linear Growth of Rapidly Deposited pH₂ Samples. Total (front+back) thicknesses are calculated from the absorption intensities of the S₁(0)+S₀(0) band integrated over the 4825 to 4855 cm⁻¹ range. The total H₂ gas inlet amounts were: 0.38 moles for the top trace, and 0.22 moles for the bottom trace. During the depositions, the BaF₂ substrate holder temperature rose from a baseline of 1.9 K, to 2.8 K and 2.5 K for the top and bottom traces, respectively.

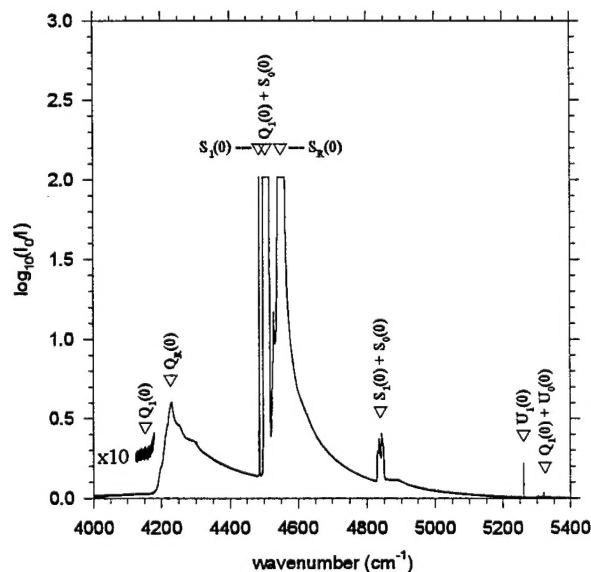


Figure 5. IR Absorption Spectrum of ≈ 6 mm Thick pH₂ Sample. The sample's growth history is shown in the top trace (open circles) of figure 4. Observation of the S₁(0) transition at 4486 cm⁻¹ combined with the non-observation of the Q₁(0) transition at 4153 cm⁻¹ demonstrates that the microscopic crystal structure is hcp δ . The spectrum is presented at 0.15 cm⁻¹ FWHM resolution, without any corrections whatsoever for optical scattering losses.

H₂ inlet rates depicted in figure 3. The observed linear growth rates and constant deposition efficiencies indicate that any additional thermal impedance due to the presence of the several millimeters thick pH₂ sample is a negligible component of the overall thermal impedance between the matrix accretion layer and the liquid helium bath.

Figure 5 shows the absorption spectrum of the same 99.99% pH₂ sample as depicted in the top trace of figure 4. At these very low oH₂ concentrations, the absorption spectrum yields quantitative information about the symmetries of the sites occupied by the pH₂ molecules. The close similarities between our observed solid pH₂ absorption lineshapes and those for large single crystal pH₂ samples [refs. 15-17] suggest that the vast majority of the H₂ molecules in our samples exist in an environment very similar in short-range structure to that found in hexagonal close-packed (hcp) pH₂ crystals[§]. More specifically: observation of the S₁(0) absorption demands the absence of inversion symmetry in the H₂ molecules' local environment, while non-observation of the Q₁(0) absorption demands that the sum of the vectors connecting each H₂ molecule with all of its nearest neighbors vanishes [ref. 18]. These observations are consistent with an hcp host structure, but not with face-centered cubic (fcc) or other centrosymmetric lattices, nor are they consistent with amorphous structures, or with the presence of large numbers of vacancy defects. We conclude that over 99.95% of the H₂ molecules in our samples exist in effectively hcp sites[§].

These spectroscopic observations, combined with the samples' excellent optical transparency and thermal properties, suggest an overall polycrystalline hcp structure[§] with fairly large (~ 1 mm ?) crystallites. We are preparing to confirm this assertion by performing visual inspections of thick vapor deposited pH₂ samples between crossed-polarizers [ref. 5].

We began studying vapor depositions of hydrogen samples in the first place to allow for the deliberate introduction of isolated energetic dopant species. Growing pH₂ crystals from the melt results in very pure samples, as few species (*e.g.*: oH₂, HD, D₂, HT, DT, T₂, and to a lesser extent: He, Ne) have any appreciable solubility in liquid pH₂, or survive phase separation upon freezing [ref. 4]. Furthermore, some reactive species are quite mobile in *solid* hydrogen at temperatures above ≈ 5 K [ref. 1] and are thus subject to loss via recombination. Fortunately, vapor deposition is an effective way of preparing doped solid samples which additionally allows us to take advantage of the myriad of dopant production techniques developed in previous matrix isolation spectroscopic studies [ref. 19].

Figure 6 shows IR absorptions of carbon clusters (and probably also hydrocarbons) trapped in a 1.2 mm thick pH_2 sample at $T = 2$ K. The signal:noise ratio of $\approx 100:1$ for the main C_3 peak is significantly improved over recently published results [refs. 7, 20]. The observed irreversible changes in the intensities of the " C_3 " peaks upon annealing to 4 K contradicts previous observations [ref. 20] and argues for the existence of multiple trapping sites for C_3 in pH_2 (or for a reassignment of the lines in the 2030 to 2040 cm^{-1} region).

Figure 7 shows broad UV absorptions centered at 209 and 217 nm which we have previously assigned to B atoms isolated in solid hydrogen [ref. 2]. This spectrum as well represents a vast improvement in signal:noise ratio over our previous efforts (the estimated B atom concentrations are still low, but the optical path lengths are ~ 10 to 100 times longer than before). The improved optical quality of our new samples should be a great help in our ongoing efforts to prove conclusively the trapping of B atoms in pH_2 .

In addition to yielding improved spectra of dopant species, the increased optical path

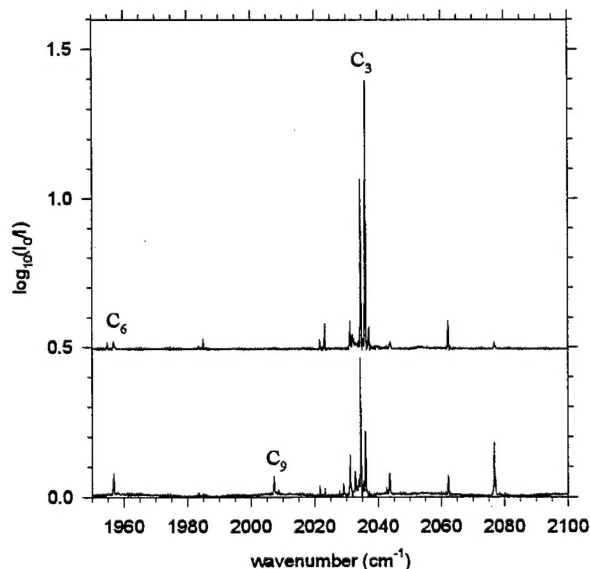


Figure 6. IR Absorptions of Carbon Clusters in pH_2 at $T = 2$ K. The sample was prepared by laser ablation of graphite. The top trace shows the as-deposited sample, with: $T = 2$ K, $\lambda_{abl} = 308$ nm, $\Phi_{abl} \approx 8 \times 10^7$ W/cm 2 , 100 mJ/pulse, 10 Hz repetition rate, 30 minute C_n deposition time, H_2 inlet flow rate ≈ 120 mmol/hr, $l = 1.2$ mm. The bottom trace shows the sample again at 2 K, after warming to 4 K. Resolution is 0.15 cm^{-1} FWHM.

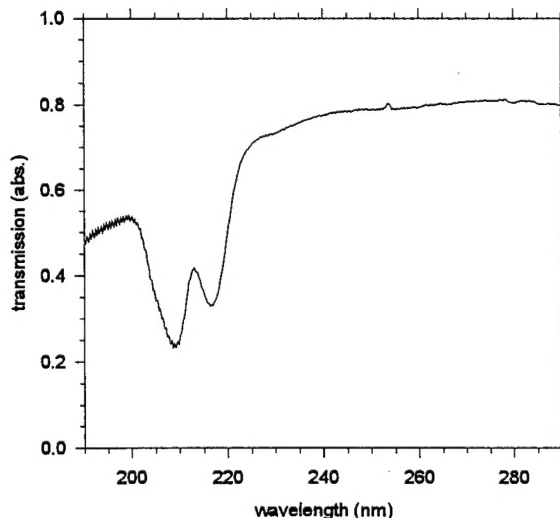


Figure 7. UV Transmission Spectrum of B/H_2 at $T = 2$ K. The sample was prepared by laser ablation of solid boron with: $T = 2$ K, $\lambda_{abl} = 308$ nm, $\Phi_{abl} \approx 9 \times 10^7$ W/cm 2 , 110 mJ/pulse, 10 Hz repetition rate, 60 minute B deposition time, H_2 inlet flow rate ≈ 55 mmol/hr, $l = 1.0$ mm.

lengths provided by our rapidly deposited samples enables us to detect the weak IR activity induced by the dopant species in the solid hydrogen host itself. Perhaps the most familiar example of this impurity-induced IR activity is that due to oH_2 impurities in pH_2 , as shown in figure 3. This effect is absent in rare gas atom host matrices, but is a topic of current interest in doped N_2 matrices [refs. 21, 22].

Figure 8 shows IR absorptions induced by the presence of neutral dopants. The complexity of the spectral pattern seems to increase as the dopant changes from atomic to diatomic to polyatomic, perhaps reflecting an increase in the number of dissimilar H_2 molecular environments. All the peaks appear within $\pm 10 \text{ cm}^{-1}$ of the position of the $\text{Q}_1(0)$ line in the 2% oH_2 sample. Figure 9 shows IR absorptions induced by charged dopants. The large decrease in absorbance near 4150 cm^{-1} is the so-called "interference" feature due to trapped excess electrons,

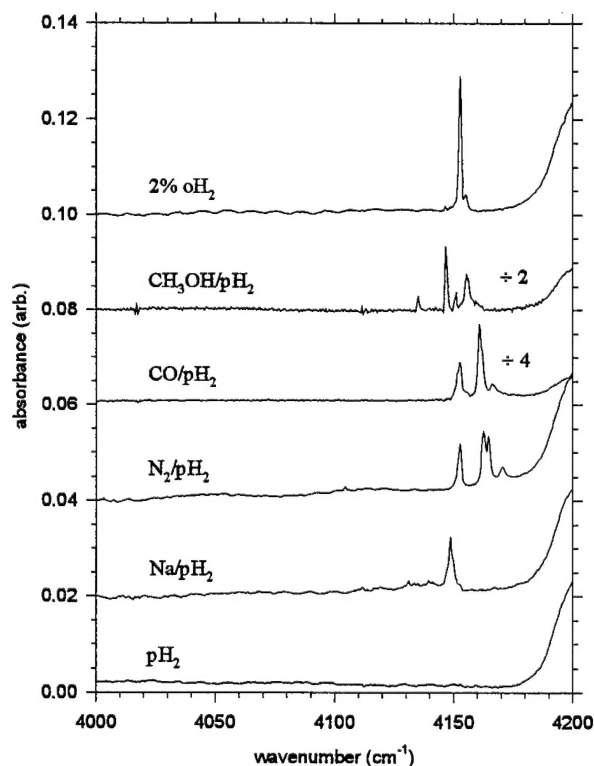


Figure 8. Neutral-Dopant Induced H_2 IR Absorptions at $T = 2 \text{ K}$. The pure pH_2 and the 2% oH_2 traces are the same data as shown in figure 3. All samples are between 0.7 and 0.9 mm thick. The Na/pH_2 sample was prepared by laser ablation with the ion rejection magnets in place.

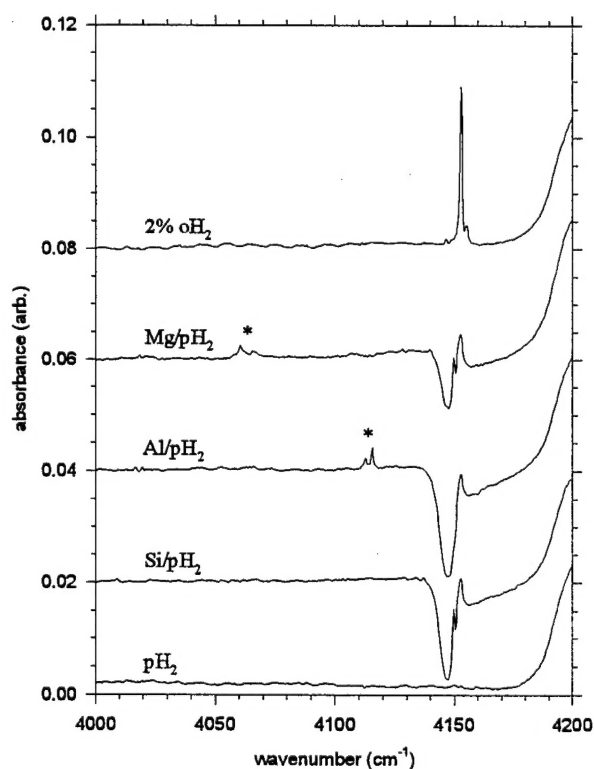


Figure 9. Charged-Dopant Induced H_2 IR Absorptions at $T = 2 \text{ K}$. All samples are between 0.8 and 1.0 mm thick. The metal doped samples were prepared by laser ablation without the ion rejection magnets. The features marked by asterisks are likely induced by positively charged species.

and is well known from studies on irradiated solid hydrogen samples [ref. 23]. The strongly red-shifted features marked by asterisks are likely due to trapped positively charged dopants, either metal ions or their reaction products. A similar positive ion induced feature has been observed at 4149.7 cm^{-1} in γ -ray irradiated $p\text{H}_2$ crystals [ref. 24]. Stark shifts for the ro-vibrational energy levels of H_2 adjacent to a positive charge have been calculated [ref. 25]; direct application of these results to the data in figure 9 yields reasonable ion- H_2 separations of 2.7 \AA and 3.2 \AA for the $\text{Mg}/p\text{H}_2$ and $\text{Al}/p\text{H}_2$ samples, respectively. Our experiments and analysis of these induced absorptions are still in progress. We ultimately expect to show that this induced IR activity can provide spectroscopic information complementary to the dopant absorptions, which will be key to the quantitative characterization of the microscopic structures of these samples.

CONCLUSIONS

We have developed a new method for rapid vacuum deposition of millimeters thick, doped, solid $p\text{H}_2$ samples. Unlike typical vacuum deposited hydrogen films, these samples exhibit very little optical scattering, even at vacuum UV wavelengths. Details of the IR absorption spectra of the pure $p\text{H}_2$ samples are consistent with an hcp crystal structure§.

The longer paths lengths afforded by this new sample preparation approach offer a significant improvement in signal:noise ratio for weak absorptions over traditional matrix isolation spectroscopy in thin rare gas host films. Additionally, IR activity induced in the $p\text{H}_2$ host by the dopants provides complimentary information about the dopant trapping environment, information unobtainable from rare gas matrix experiments.

REFERENCES

1. M.E. Fajardo, J. Chem. Phys. **98**, 110 (1993).
2. M.E. Fajardo, S. Tam, T.L. Thompson, and M.E. Cordonnier, Chem. Phys. **189**, 351 (1994).
3. S. Tam and M.E. Fajardo, unpublished B, Mg, and Al matrix isolation data.
4. P.C. Souers, Hydrogen Properties for Fusion Energy (University of California Press, Berkeley, 1986).
5. I.F. Silvera, Rev. Mod. Phys. **52**, 393 (1980).
6. M.E. Fajardo, M. Macler, and S. Tam, "Progress Towards Deposition of Velocity Selected Aluminum Atoms into Cryogenic para-Hydrogen Matrices" in Proceedings of the High Energy Density Matter (HEDM) Contractors' Conference held 5-7 June 1996 in Boulder CO, ed. P.G. Carrick and N.T. Williams, PL-TR-96-3037 (Phillips Lab, Edwards AFB, CA, 1997).

7. S. Tam, M. Macler, and M.E. Fajardo, *J. Chem. Phys.* **106**, 8955 (1997).
8. M. Born and E. Wolf, Principles of Optics, 6th edition (Pergamon Press, Oxford, 1987).
9. M. Macler and M.E. Fajardo, *MRS Symp. Proc.* **285**, 105 (1993).
10. M. Macler and M.E. Fajardo, *Appl. Phys. Lett.* **65**, 159 (1994).
11. M. Macler and M.E. Fajardo, *Appl. Phys. Lett.* **65**, 2275 (1994).
12. M. Macler and M.E. Fajardo, *MRS Symp. Proc.* **388**, 39 (1995).
13. J. Van Kranendonk, *Physica* **23**, 825 (1957).
14. J. Van Kranendonk and G. Karl, *Rev. Mod. Phys.* **40**, 531 (1968).
15. H.P. Gush, W.F.J. Hare, E.J. Allin, and H.L. Welsh, *Can. J. Phys.* **38**, 176 (1960).
16. A. Crane and H.P. Gush, *Can. J. Phys.* **44**, 373 (1966).
17. S.Y. Lee, Ph.D. thesis, The Ohio State University (1987).
18. J. Van Kranendonk and H.P. Gush, *Phys. Lett.* **1**, 22 (1962).
19. D.W. Ball, Z.H. Kafafi, L. Fredin, R.H. Hauge, and J.L. Margrave, A Bibliography of Matrix Isolation Spectroscopy 1954-1985 (Rice University Press, Houston, TX, 1988).
20. M. Miki, T. Wakabayashi, T. Momose, and T. Shida, *J. Phys. Chem.* **100**, 12135 (1996).
21. D.P. DiLella and D.E. Tevault, *Chem. Phys. Lett.* **126**, 38 (1986).
22. F. Legay and N. Legay-Sommaire, *J. Phys. Chem.* **99**, 5277 (1995).
23. S.K. Bose and J.D. Poll, *Can. J. Phys.* **65**, 58 (1987).
24. T. Momose, K.E. Kerr, D.P. Weliky, C.M. Gabrys, R.M. Dickson, and T. Oka, *J. Chem. Phys.* **100**, 7840 (1994).
25. J.D. Poll and J.L. Hunt, *Can. J. Phys.* **63**, 84 (1985).

§ Addendum

Discussions with other members of the HEDM community brought to our attention a flaw in our arguments for a nearly pure hcp structure. Our IR absorption spectra demonstrate the presence of some hcp pH_2 , but do not preclude the presence of fcc or random-stacked close packed structures. Since the 1997 conference we have recorded the spontaneous Raman scattering spectrum of our rapidly deposited samples. These new data show that the as-deposited microscopic structure is in fact a mixture of fcc and hcp, with the possible inclusion of random-stacked close packed structures as well. These observations are in complete agreement with the results reported by Collins, et al., *Phys. Rev. B* **53**, 102 (1996).